Crack growth behavior of aluminum alloy 6061 T651 under uniaxial and biaxial planar testing condition

S. Henkel, E. Liebelt, H. Biermann, S. Ackermann
Institute of Materials Engineering, Technische Universität Bergakademie Freiberg, Gustav-Zeuner-Str. 5, 09599 Freiberg, Germany
henkel@ww.tu-freiberg.de

L. Zybell
Institute of Mechanics and Fluid Dynamics, Technische Universität Bergakademie Freiberg, Lampadiusstraße 4, 09599 Freiberg, Germany

ABSTRACT. The crack growth behavior of the aluminum alloy 6061 T651 was investigated using cruciform specimens with a measurement area of 120 x 120 x 2 mm^3 with two center crack configurations of the starting notch parallel to one of the loading axes and under an angle of 45°, respectively. For the case with crack direction in one of the loading axes the load ratio $R = \sigma_{min} / \sigma_{max}$ as well as the force parallel to the crack direction (resulting in different T-stresses) were changed. Crack growth rate was studied under varying T-stress. Also the retardation after single overloads was determined for R = 0.1, R = 0.5 and R = 0.8. As a result a change in T-stress does not significantly affect crack growth rate on high R ratios (R = 0.5) for constant ΔF loading. In case of lower R-ratios (R = 0.1) crack growth retardation was observed at presence of a static tensile load parallel to the crack growth direction due to higher influence of crack closure. Furthermore, such tensile load results in longer retardation periods after applying an overload at R = 0.1. Less pronounced overload retardation can be assumed with tensile force FX for R = 0.8 and 1.3 times overloads.
Non proportional loading with a phase shift in time between the two axes of 45° and 90° results in a mixed mode situation (mode I / mode II) at the crack tip of a crack which is orientated under 45° to the loading axes. Mode I and mode II fractions change during every cycle. A phase change of 45° did not change crack growth significantly compared with proportional load. Crack branching occurred when changing from proportional loading to non-proportional 90° phase shifted loading. The two crack tips of the center crack under 45° divided in 4 crack tips under approximately 90° to the loading axes which were simultaneous propagating for more than 10 mm. Finally, two crack tips propagated faster than the remaining two.
The stress intensity factors K_I and K_{II} as well as the T-stress where calculated by FEA (ABAQUS). For the 45° crack orientation and the non-proportional load case with 90° phase shift linear elastic FEA calculations show that there are time dependent rotating principal stress axes on the crack tip during one cycle. In the unnotched (uncracked) specimen there are fixed principal stress axes also in the phase shifted loading case. The configuration with 4 cracks has a significant higher ΔK_I than the configuration with two crack tips while ΔK_{II} is significantly lower.
In addition uniaxial crack growth measurements were performed on SENB specimen in the size of 10 x 20 x 100 mm^3 covering the threshold and Paris-region for loading ratios R = 0.1, 0.3, 0.5, 0.8.

KEYWORDS. Fracture mechanics; Fatigue; Crack growth; Cruciform sample; Crack branching.

INTRODUCTION

It is known from literature that the nonsingular T-stress parallel to a crack surface influences the shape and the size of the plastic zone at the crack tip [1]. The standard specimens for fracture mechanics testing have different in plane constraint conditions depending on specimen type and crack length [2]. Therefore, in static testing the shape of the static crack resistance curve depends on specimen type [3] and crack length to ligament ratio is limited by standards as ASTM E1820. There are also measurements in literature, which found an influence of T-stress on fatigue crack growth by using different specimen types [4] or cruciform samples in planar biaxial loading [5, 6].
Dalle Donne et al. [7] showed that the shape of the cruciform sample is important for a proper measurement and there is a lot of misunderstanding due to specimen effects, which are treated as material behavior because an uncoupled loading in the two loading axes is possible only for a specimen with long slits. Today, there is also the possibility to consider the coupling effect by finite element analysis. Sunder and Ilchenko tested random flight spectrum load on cruciform specimens from aluminum alloy 2024-T3 with and without phase shift in time between the loading axes and crack direction in the direction of one axis. They showed that considering the coupling between the load axes ΔK is a proper parameter to describe the fatigue crack growth [8].
The aim of the present study is to clarify if there is an effect of crack parallel tensile forces, which affect the T-stress on fatigue crack growth in a common aluminum alloy. Regarding the size and the shape of the plastic zone, overload effects are taken into account because the retardation after overloads depends on the plastic zone, which is formed by overload cycles [9].

MATERIAL AND METHODS

The investigated material was the aluminum alloy 6061 (EN AW-AlMgSi1Cu) in the condition T651 (solution annealed, quenched, controlled strained and artificially aged). The material had a chemical composition of 0.76% Mg, 0.56% Si, 0.23% Cu, less than 0.7% Fe. The samples were milled out of a 13 mm thick plate. The mechanical properties of the static tensile test as well as the fracture mechanics parameter for stable crack initiation $J_{i/BL}$ calculated from the intersection of the blunting line and the static crack resistance curve from SENB specimen with 10x20x100mm³ are given in Tab. 1. For comparison with the K based loading in the cyclic tests the elastic recalculated $K_{Ji/BL}$ is also given. The microstructure (given in Fig. 1a) contains precipitates which are arranged in lines parallel to the rolling direction. The samples where cut under an angle of 45° to this direction.
Fig. 1b shows the cyclic crack growth curves for the material at $R = \sigma_{min} / \sigma_{max} = 0.1$; 0.3; 0.5 and 0.8, respectively. The measurements were done on SENB specimens (10 x 20 x 100 mm³) according to ASTM E647 [10] using an electrodynamic resonance testing system RUMUL Mikrotron with 20 kN maximum capability. The threshold area was measured with ΔK decreasing and the Paris region with ΔK increasing. Notch orientation was 45° to the rolling direction, that means between L-T and T-L orientation. Crack length measurement was done by elastic compliance method. The test frequency was between 65 Hz and 77 Hz. The scatter was reduced using 7 point polynomial method according to ASTM E647 [10]. The material shows the well-known point of inflection in the transition to the Paris region [11], which is caused mainly by switching to grain surface oriented crack growth [12]. There is a difference in crack growth rate especially at low R-values, between ΔK increasing and decreasing due to load history effects and crack closure.

Direction	$R_{p0.2}$ [MPa]	R_m [MPa]	A_g [%]	A_5 [%]	$J_{i/BL}$ [kJ/m²]	$K_{Ji/BL}$ [MPa√m]
L-T	282	319	10.5	18.1	69	98
T-L	275	321	9.3	14.5	48	82

Table 1: Mechanical properties of the static tensile test as well as the fracture mechanics parameters for stable crack inition $J_{i/BL}$ calculated from the intersection of the blunting line and the static crack resistance curve.

The planar biaxial tests were done using a slotted cruciform specimen with thinned inner measurement area which is shown in Fig. 2a). This type of specimen which was developed in [13] shows an excellent uncoupling between stresses in both principal directions in the center due to the slits [14]. Avoiding notch effects on the end of the slits, the slits were

made with radii, which reduce the load carrying area of the loading arms. Therefore, the measurement area is reduced in thickness to get higher stresses there. The notch was induced by electro discharge machining. For small crack sizes the behavior of the specimen is near to the infinite plate. Loading only the Y-axis, the specimen with the crack configuration shown in Fig. 2a is quite comparable to the center crack tension (CCT) specimen. A negative T-stress is resulting [15]. An additional tensile loading in X-direction results in a shift of the T-stress to positive direction. Fig. 2b shows the T-stress based biaxiality ratios β versus the normalized crack size a/W for different standard specimen geometries [2] and the principle possible variation within the cruciform specimen.

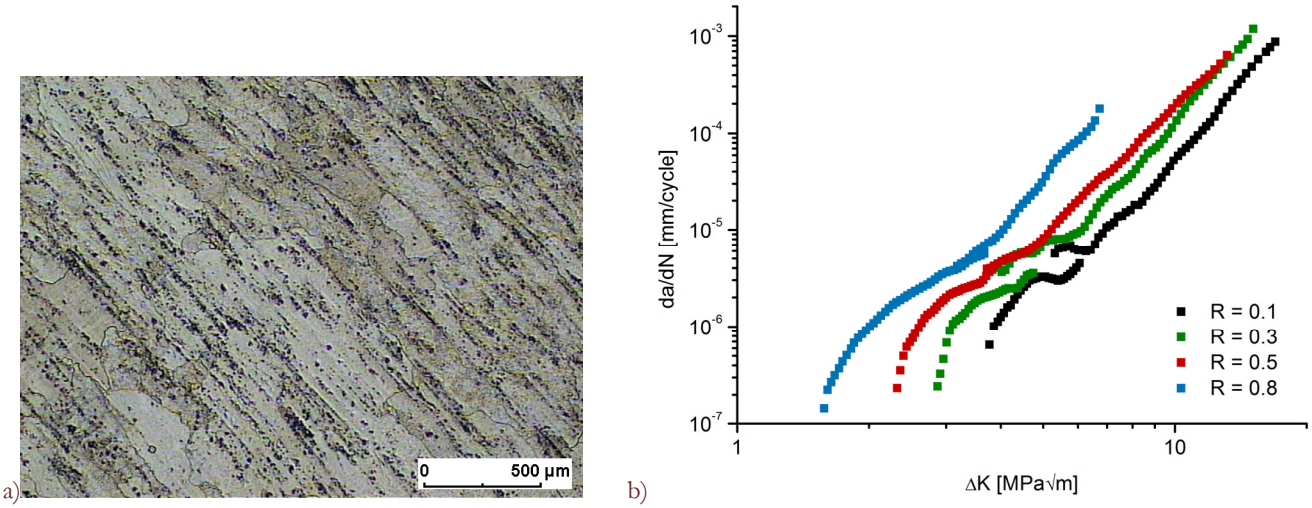

Figure 1: a) Microstructure of the tested aluminum alloy 6061 T651: Precipitates arranged in lines parallel to the rolling direction. b) Crack growth curves for different load ratios $R = \sigma_{min} / \sigma_{max}$ measured on SENB specimens.

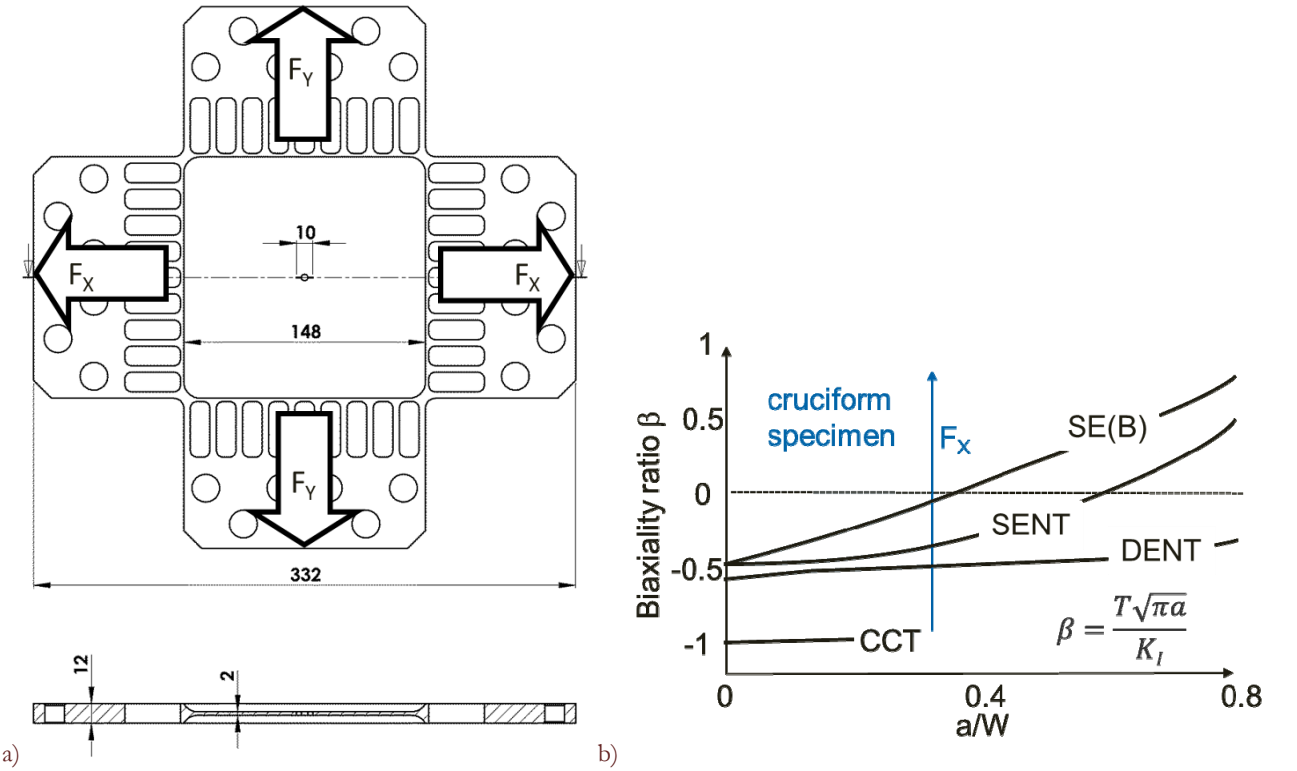

Figure 2: a) Cruciform specimen with slotted arms and thinned inner measurement area together with the loading directions F_X and F_Y (dimensions in mm). b) Biaxiality ratio β depending on crack length to ligament ratio for different standard specimens [2] and the cruciform specimen with variation of F_X.

For a crack oriented 45° to the loading axes (Fig. 3a), there could also be a change in the crack opening mode if a phase shift in time between the cyclic loads of both axes is applied. For a proportional load with equal amplitudes in both axes, pure mode I exists. For a phase shift of 180° it is pure mode II. Phase shifts between 0° and 180° cause changing mode I and mode II ratios during every cycle. For a phase shift of 90° and tension-tension load, Fig. 3b shows the K_I and K_{II} development during one complete cycle. Fig. 3c shows schematically the von Mises stress distribution on the crack tip during this cycle calculated by FEA for a completely elastically calculated material behavior without a hardening rule. It was found that also the principle stress axes rotate locally on the crack tip while the principle stress axes in an unnotched cruciform specimen remains fixed also for phase shifted load cases. As there are LCF conditions within the plastic zone, non proportional hardening effects have to be taken into account. Itoh et al. [16] showed only a small effect of rotating principal stress axes on LCF lifetime for the Aluminum alloy 6061.

The experiments were carried out on a servo-hydraulic planar biaxial testing system Instron with a maximal force of 250 kN. The geometry function for the stress intensity factor and the level of T-stress as a function of crack length and external loads were calculated by elastic FEA using the ABAQUS program. The crack lengths were determined using the indirect potential drop method with crack gages (range 20 mm) and a FRACTOMAT of the company Russenberger. In each case, one crack gage per crack end was used. The load was applied under force control with a frequency of 20 Hz with blockwise constant load or single overloads. For the notch in load direction (Fig. 2a), the fatigue load was applied by the force F_Y (perpendicular to the crack) and F_X (parallel to the crack) was varied between 0 and 40 kN as a non-cyclic static load. In this case, a load of 40 kN corresponds to a stress of σ_Y = 118 MPa in the center of the uncracked specimen. Without a load in X-direction, a negative (compressive) cyclic T-stress is resulting, which is shifted with additional stress in X-direction into positive region. A blockwise variation of the phase between the loading axes was applied at equal load amplitude ($F_{Xa} = F_{Ya}$ = 6,16 kN, R = 0.5) and frequencies in both axes for the 45° notch. The starting notch for this case was perpendicular to the rolling direction.

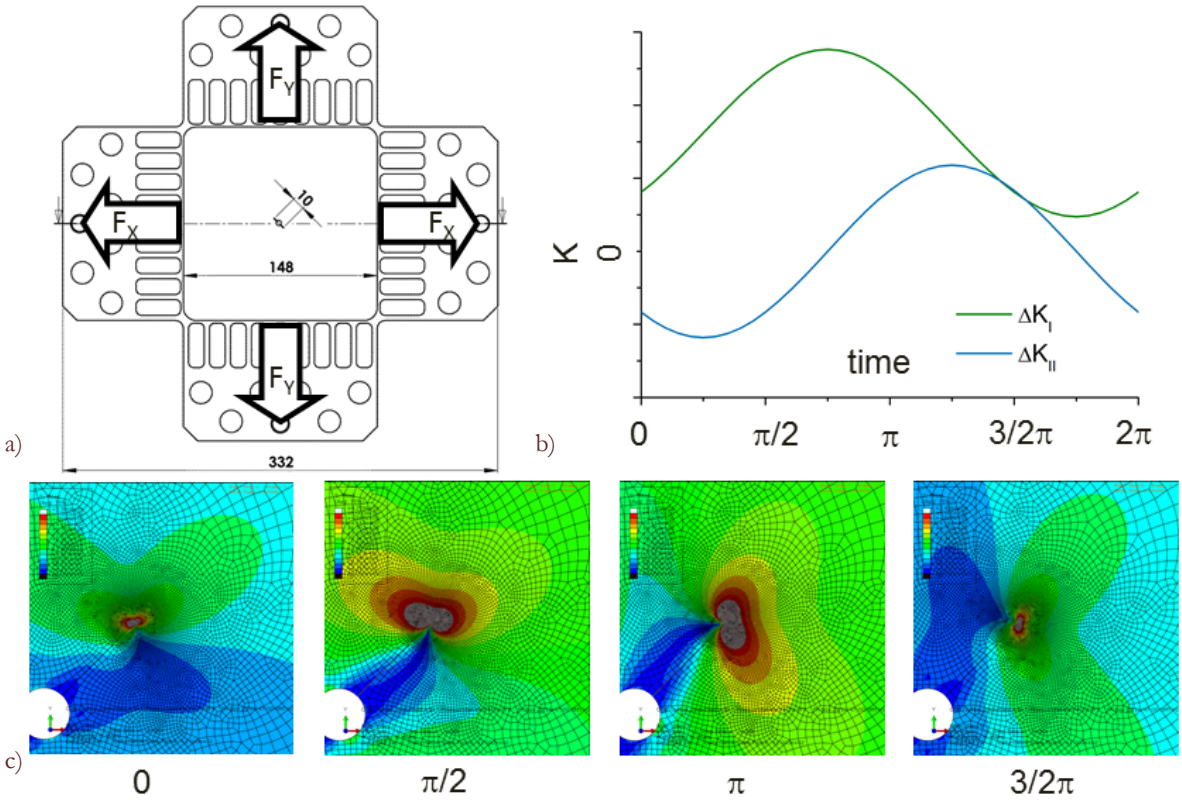

Figure 3: a) Crack configuration 45° to the loading axes, b) elastically calculated crack tip parameters K_I and K_{II} on a 45° crack configuration and 90° phase shifted loading for positive R-ratio, c) change in shape of the von Mises stress distribution on this crack configuration (elastic FEA).

RESULTS AND DISCUSSION

In the biaxial tests without overload, only a small influence of a block-wise or continuously modified loading F_X parallel to the crack on the crack growth rate was found. Fig. 4 shows the crack growth data in comparison with the stress intensity parameter ΔK. For comparison the crack growth values and the scatter band [17] of the uniaxial measurements on the SENB samples are given. For R = 0.1 (Fig. 4a) it was attempted to reduce the load to a ΔK-value of 8 MPa√m at the beginning of each block. In order to minimize load history effects the further crack growth was carried out under constant force amplitude F_{Ya} at blockwise variation of the static load Fx. In this measurement, the crack growth rate is lower for tensile load in the crack direction X. Probably crack closure effects such as roughness, for example, or plasticity induced crack closure is supported by a T-stress shifted to the tensile region. For the crack growth data at R = 0.5 shown in Fig. 4b), the influence of the variation of T-stress is significantly lower and mostly within the uniaxial scatter band. The gray line in this picture shows data for a continuous ramping in F_X while cyclic loading in F_Y.

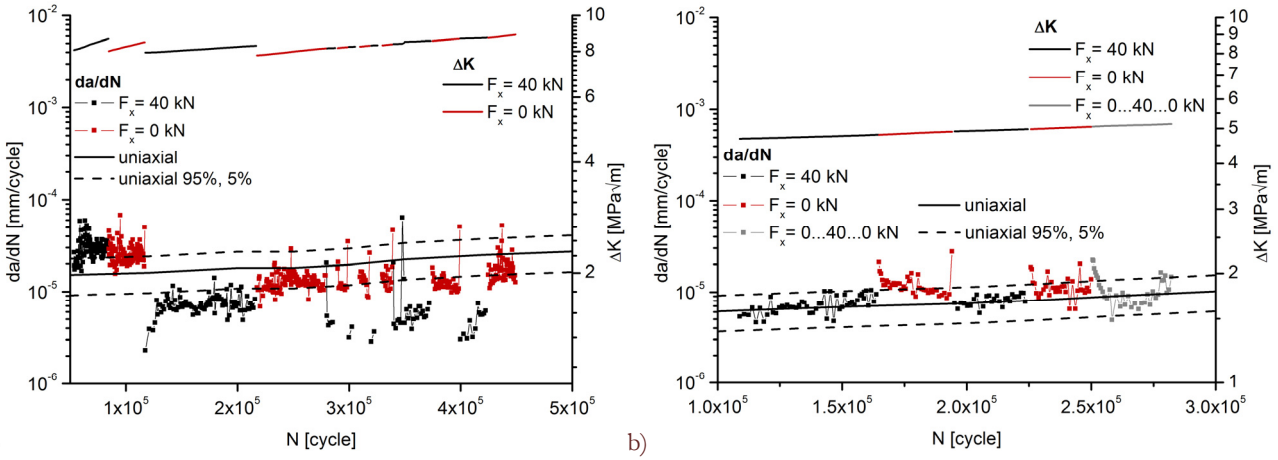

a) b)

Figure 4: Crack growth rates and cyclic stress intensity factors ΔK versus number of cycles under variation of the force parallel to the crack F_X for a) R = 0.1 and b) R = 0.5.

Fig. 5 shows the average crack length measurement signals of the two crack gages versus cycle number (Fig. 5a) and the corresponding crack growth rates (Fig. 5b) for two consecutive 1.5-fold overloads with approximately the same load at R = 0.5 with and without load in the crack direction F_X. The delay before the crack growth rate has returned to the initial level is approximately 103,200 cycles for F_X = 40 kN and 77,500 cycles for F_X = 0 kN.

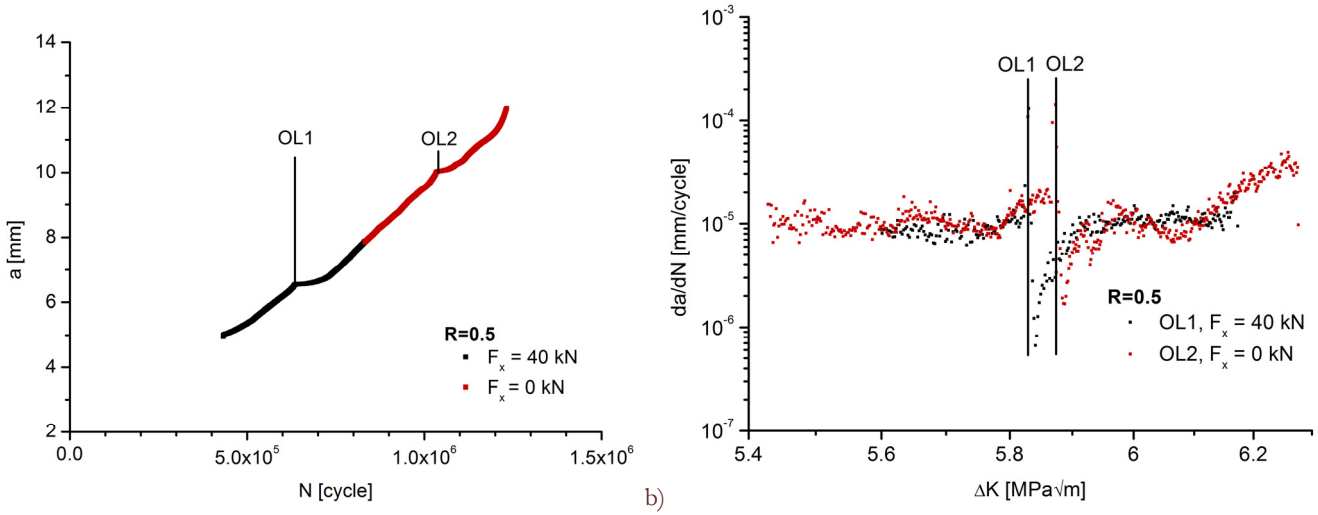

a) b)

Figure 5: a) Averaged crack length signal of the two gages versus cycle for two 1.5-fold overloads at R = 0.5 with variation of the force parallel to the crack Fx, b) crack growth rate versus ΔK for the two overloads.

More pronounced difference was found at R = 0.1 shown in Fig. 6. The crack length signals and the crack growth rates of five consecutive 1.5-fold overloads are shown. The overloads, in which the sample was loaded with 40 kN tensile force in the X-direction, show a significant increase in the delay effect until the original crack growth rate is achieved again. It rises to about 1.5 ... 1.8 times comparing with the overloads with F_X = 0 kN

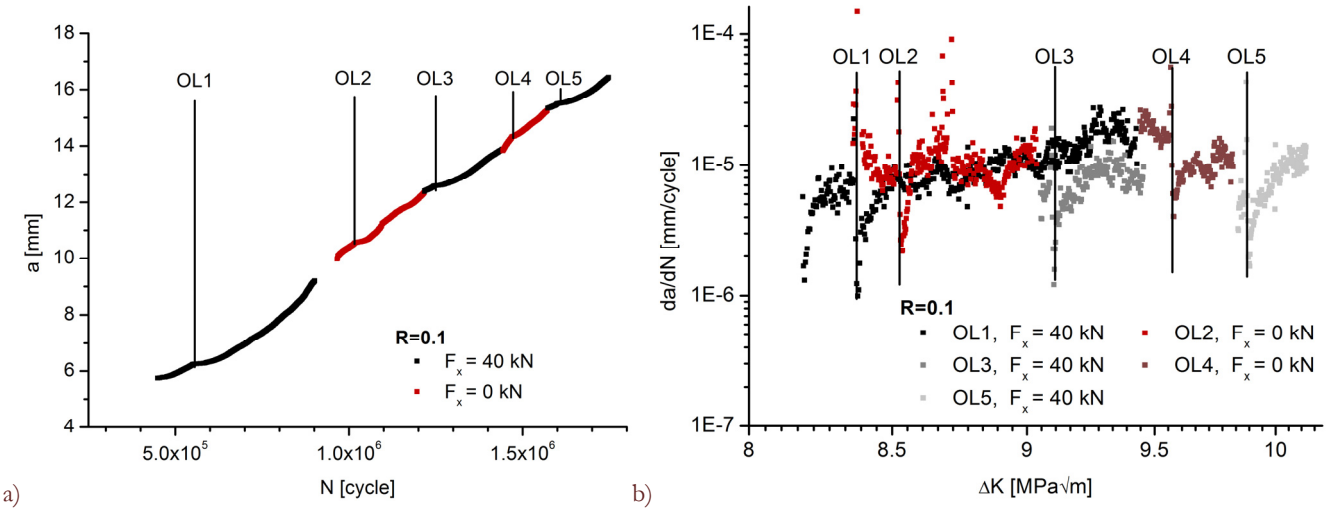

a) b)

Figure 6: a) Averaged crack length signal of the two gages versus number of cycle for fife 1.5-fold overloads at R = 0.1 with variation of the force parallel to the crack F_X, b) crack growth rate versus ΔK for these overloads.

For high static preloads at R = 0.8 the corresponding tests are not suitable to detect a clear tendency of the influence of crack parallel stress. Fig. 7 shows the development of the crack gage signal and crack growth rates for one single crack tip for a test with constant load amplitude F_Y and eight 1.3-fold overloads with varying F_X. The other crack tip kept nearly completely arrested after the first overload, so the crack size became asymmetric. The objective to obtain a significantly larger crack propagation between the overloads as the estimated size of the plastic zone (Dugdale) $d_{pl} = \frac{\pi}{8}\left(\frac{K_{Imax}}{R_{p0.2}}\right)$ [18] was not fully achieved in this experiment. If the plastic zone of the base load is subtracted it is fulfilled. The results suggest in contrast to the experiments at R = 0.1 a slight reduction in delay with tensile loading in X-direction. That might be caused by a reduction in plastic zone size due to higher in plane constraint.

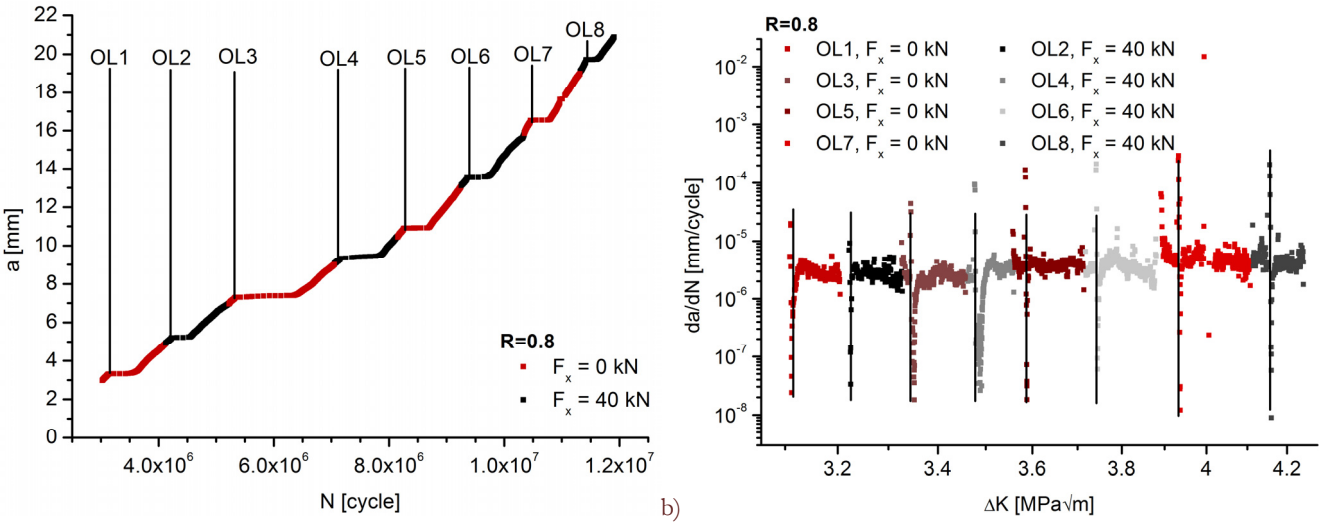

a) b)

Figure 7: a) Crack length signal of the one crack gages versus cycle for 1.3-fold overloads at R = 0.8 with variation of the force parallel to the crack F_X, b) crack growth rate versus ΔK for these overloads.

Fig. 8 shows the retardation cycles after the overloads for the tested samples. A tendency was observed that the overload delay of crack growth is higher at R = 0.1 with a force F_X = 40 kN parallel to the crack while at R = 0.5 and R = 0.8 it is equal or lower.

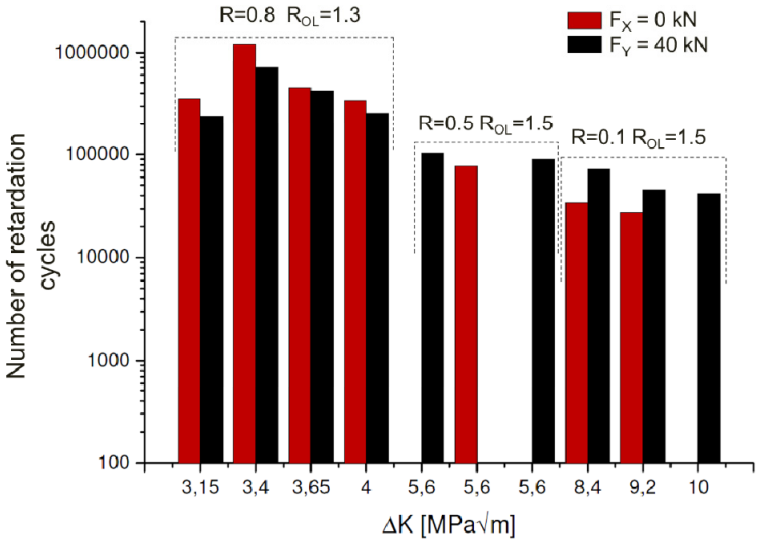

Figure 8: Crack retardation for the tested overloads depending on R-ratio and loading parallel to the crack growth direction.

For the starting notch with an orientation of 45° to the loading axes the crack tips propagate straight forward. A change to 45° phase shift between the sine functions for 100,000 cycles did not result in a change in crack growth rate. After changing from proportional loading to 90° phase shifted loading the two crack tips branched after a short incubation period app. 45° to the starting notch direction (Fig. 9). All four cracks propagated simultaneously. The crack length measurement with the crack gage is not valid from this point because the electric resistance is changing more with the two branched cracks on each gage and the two crack lengths cannot be separated. Therfore, further measurements were done with a high resolution camera system [19]. Between both measurements is a gap because crack branching was not expected.

Fig. 10 shows the crack length for the two crack tips (signals of the crack gages) and four crack tips from the camera measurements versus number of cycles. Crack branching occurred at app. 0.63 million cycles. It can be seen that all four crack tips propagated quite simultaneously until 1.6 million cycles. From that time a pair of two cracks grow faster than the other ones (Fig. 9).

Similar crack branching was found by Mall and Perel [20] for the aluminum alloy 7075 T6 for 90° and 180° phase shifted loading of a cruciform specimen with starting crack position 45° to the loading arms. The authors found by FEA calculations that the sum of the strain energy release rates of the two split cracks is equal to that of a single crack under biaxial fatigue without a phase shift.

A principal understanding for that branching can be given by calculating the stress intensity factors for a configuration with two cracks compared to a branched configuration in Fig. 11. Due to the symmetry of the cracks only one end or one pair of branched crack tips are shown. Comparing the time dependent mode I and mode II fractions it can be seen that for each of the four branched crack tips in Fig. 11a the ΔK_I has a significant higher value, than for the unbranched configuration with two crack tips shown in Fig. 11b. The mode II ΔK_{II} is significantly lower for the branched configuration.

The used FEA model does not consider crack surface contact and calculates therefore negative mode I stress intensity factors K_I which are not possible in the real configuration.

Figure 11c in addition to Fig. 3c shows the von Mises stress field on the two branched crack tips during one cycle. Both cracks ends are opened time shifted in mainly mode I.

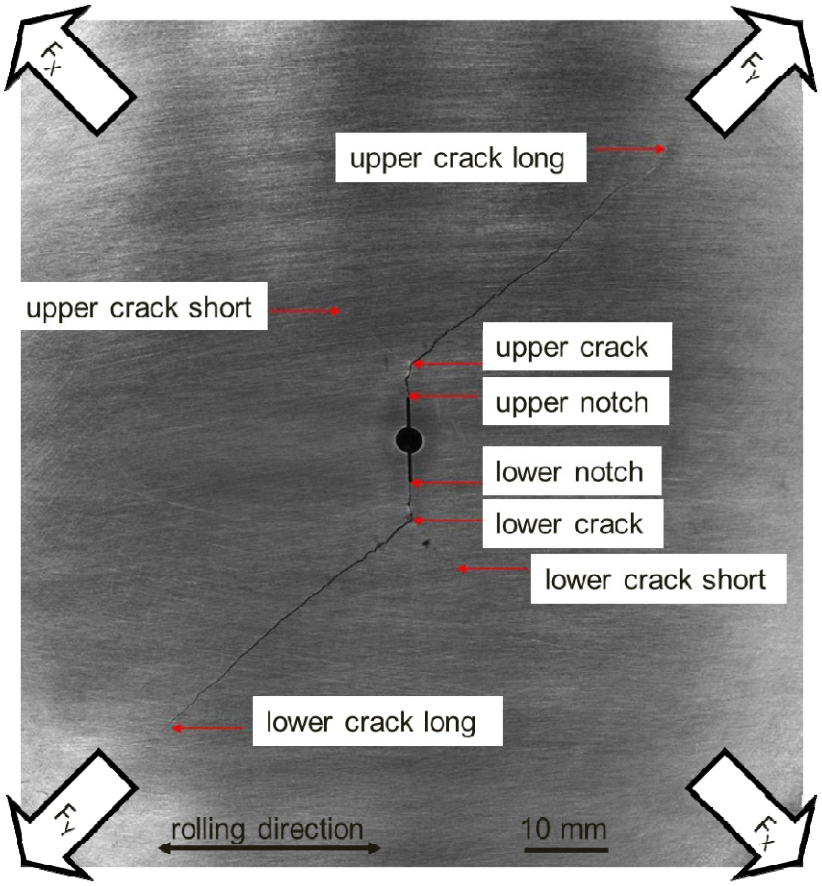

Figure 9: Crack path for the 45° turned notch and loading directions. After changing to 90° phase shift the two crack tips branched into four crack tips. Two of them (marked as upper crack long and lower crack long) propagate faster than the other.

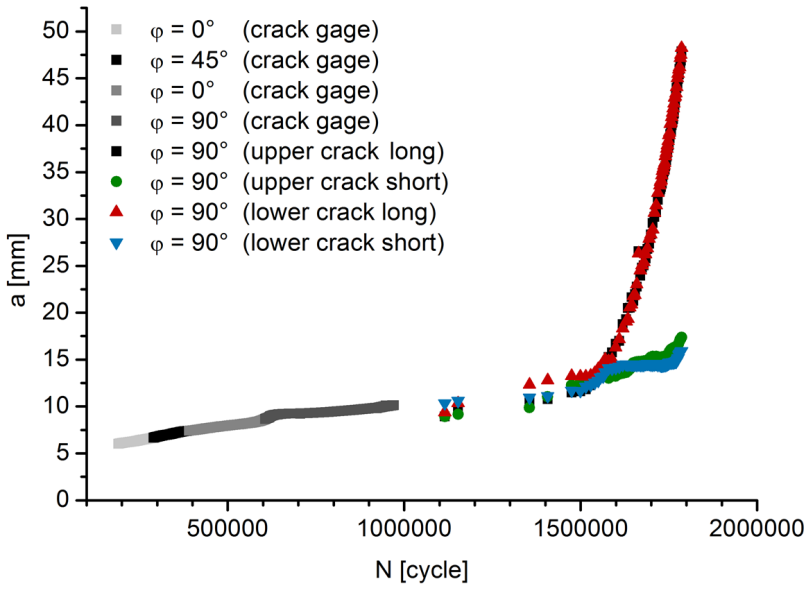

Figure 10: Crack length a versus number of cycles for the crack tips. Measurements were carried out with crack gage before and with camera system and after branching.

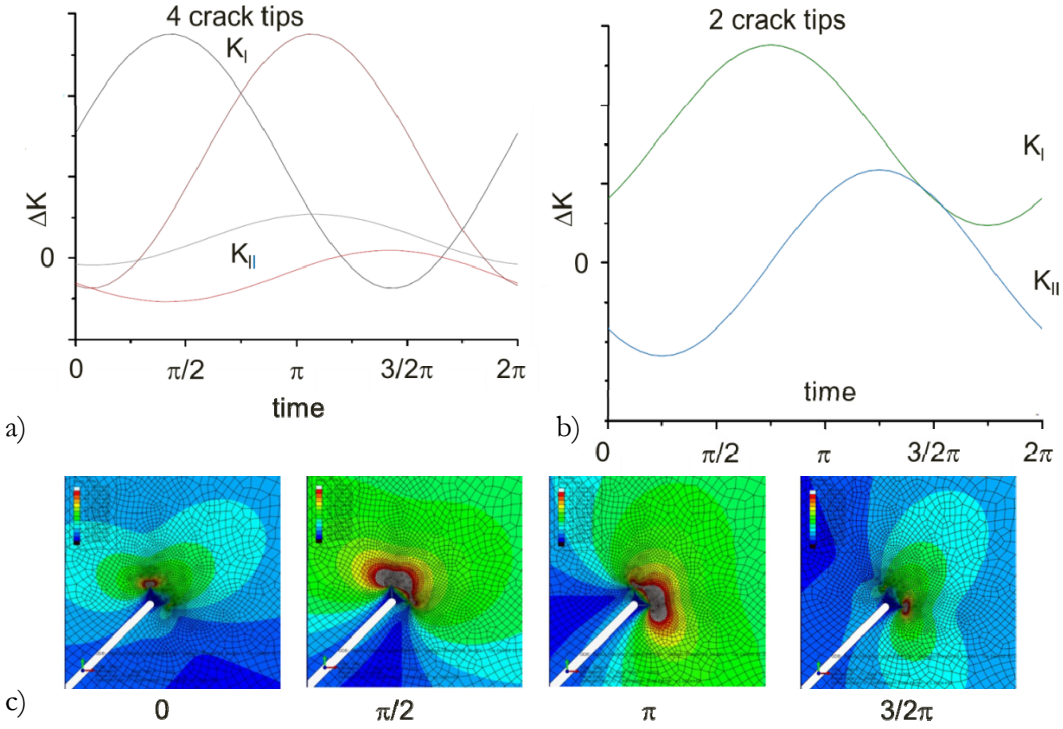

Figure 11: Comparison of configurations with two and four (branched) crack tips with linear elastic FEA. a) Time dependent change in stress intensity factors K_I and K_{II} for four crack tips. b) Stress intensity factors for two crack tips, c) von Mises stress distribution for a branched crack configuration.

SUMMARY AND CONCLUSIONS

The influence of an additional tensile load parallel to the crack propagation direction on the fatigue crack growth was investigated. In the examined stress intensity factor range, only a small influence of a crack parallel load F_X = 40 kN was detected for the fatigue crack growth at a constant load amplitude in the aluminum alloy 6061 T651. At R = 0.1 a slightly lower crack growth rate was found with the tensile load F_X.

The known retardation in the overload case was found. The tensile load in crack direction F_X caused a significant longer retardation by a factor of about 1.5 to 1.8 for 1.5 times overloads at R = 0.1.

For the loading with and without overload, these effects are not pronounced at R = 0.5. It seems that this effect is primarily caused by a gain of crack closure effects caused by positive T-stresses. However, the influence of crack length and previous overload, was not yet considered. Less pronounced overload retardation can be assumed with tensile force F_X for R = 0.8 and 1.3 times overloads.

In principle, numerous mechanisms lead to delay after overloads [21], which are all more or less influenced by a crack parallel load (crack blunting, crack deflection, crack branching, formation of secondary cracks, strain hardening and residual stresses ahead of the crack tip, roughness and plasticity-induced crack closure). To evaluate the influence of individual factors further analysis and investigations are necessary.

Crack branching was observed for a crack aligned under 45° to the loading axes and 90° phase shifted loading between the load axes. The branched cracks propagated nearly perpendicular to the loading axes which can be understood as a crack direction with high mode I fraction.

ACKNOWLEDGMENT

The authors thank the AMAG rolling GmbH, Austria for supporting the aluminum material.

REFERENCES

[1] Matvienko, J.G., The effect of the non-singular T-stress components on crack tip plastic zone under mode I loading, Procedia Materials Science, 3 (2014) 141-146.

[2] Anderson, Ted. L., Fracture mechanics, fundamentals and applications, 3rd ed., Tayler & Francis, Boca Raton, (2005).

[3] Roos, E., Grundlagen und notwendige Voraussetzungen zur Anwendung der Risswiderstandskurve in der Sicherheitsanalyse angerissener Bauteile, Fortschritt-Berichte VDI. Reihe 18, Mechanik/Bruchmechanik, Band 122, (1993).

[4] Varfolomeev, I., Luke, M., Burdack, M., Effect of specimen geometry on fatigue crack growth rates for the railway axle material EA4T, Engineering Fracture Mechanics, 78 (2011) 742-753.

[5] Shercliff, H. R., Fleck, N. A., Effect of specimen geometry on fatigue crack growth in plane strain – II. Overload response, Fatigue & Fracture of Engineering Materials & Structures, 13 (1990) 1460-2695.

[6] Hoshide, T., Tanaka, K., Yamada, A., Stress-ratio effect of fatigue crack propagation in a biaxial stress field, Fatigue & Fracture of Engineering Materials & Structures, 4 (1981) 1460-2695.

[7] Dalle Donne, C., Trautmann, K.-H., Amstutz, H., Cruciform sprcimens for in-plane biaxial fracture, deformation and fatigue testing, in S. Kalluri, P. J. Bonacuse (Eds.), Multiaxial Fatigue and Deformation: Testing and Prediction, ASTM STP 1387, American Society for Testing and Materials, West Conshohocken, (2000) 405-422.

[8] Sunder, R., Ilchenko, B.V., Fatigue crack growth under flight spectrum loading with superposed biaxial loading due to fuselage cabin pressure, International Journal of Fatigue, 33 (2011) 1101-1110.

[9] Veccnio, R.S., Hertzberg, R.W., Jaccard R., Overload induced crack growth rate attenuation behavior in aluminum alloys, Scripta Metallurgica, 17 (1983) 343-346.

[10] ASTM E647-13ae1, Standard Test Method for Measurement of Fatigue Crack Growth Rates, ASTM International, West Conshohocken, (2013).

[11] Sandner, M., Sicherheit und Betriebsfestigkeit von Maschinen und Anlagen: Konzepte und Methoden zur Lebensdauer-Vorhersage. Springer-Verlag, Berlin, (2008).

[12] Hübner, P., Gärtner, S., Pusch G., Holze, J., Einfluss des Gefüges auf die Risswachstumseigenschaften einer AlMgSi1 Legierung, 31. Tagung DVM Arbeitskreis Bruchvorgänge, Darmstadt, DVM-Band, 231 (1999) 297-305.

[13] Brown, M.W., Miller, K.J., Mode I fatigue crack growth under biaxial stress at room and elevated temperature, in K.J. Miller, M.W. Brown (Eds.), Multiaxial Fatigue, American Society for Testing and Materials, ASTM STP 853 (1985) 135-152.

[14] Mönch E., Galster, D.: A method for producing a defined uniform biaxial tensile stress field, British Journal of Applied Physics, 14 (1963) 810-812.

[15] Sherry, A. H., France, C. C., Goldthorpe, M. R.,Compendium of T-stress solutions for two and three dimensional cracked geometries, Fatigue & Fracture of Engineering Materials & Structures, 18 (1995) 1460-2695.

[16] Itoh, T., Nakata, T., Sakane, M., & Ohnami, M., Nonproportional low cycle fatigue of 6061 aluminum alloy under 14 strain paths, in Proceedings of the 5th International conference on biaxial/multiaxial fatigue and fracture, Krakow Poland, (1997) 173-187.

[17] Hübner, P., Pusch, G., Zerbst, U., Henkel, S., Wie genau müssen zyklische Risswachstumsdaten sein? Quantilrisswachstumskurven von Konstruktionswerkstoffen, in F.J. Schmidt (Ed.) Anwendungen und Fortschritte in der Bruch- und Schädigungsmechanik, (2009) 39-49.

[18] Kuna, M., Numerische Beanspruchungsanalyse von Rissen, Springer Verlag, Berlin, (2009).

[19] Henkel, S., Holländer, D., Wünsche, M., Theilig, H., Hübner, P., Biermann, H., & Mehringer, S., Crack observation methods, their application and simulation of curved fatigue crack growth. Engineering Fracture Mechanics, 77 (2010) 2077-2090.

[20] Mall, S., Perel, V.Y., Crack growth behavior under biaxial fatigue with phase difference, International Journal of Fatigue, 74 (2015) 166-172.

[21] Sadananda, K., Vasudevan, A.K., Holtz, R.L., Lee, E.U., Analysis of overload effects and related phenomena, International Journal of Fatigue, 21 (1999) 233-246.